

SCIENTIFIC REPORTS



OPEN

Multiple stochastic pathways in forced peptide-lipid membrane detachment

Milica Utjesanovic¹, Tina R. Matin^{1,2}, Krishna P. Sigdel^{1,3}, Gavin M. King^{1,4} & Ioan Kosztin¹

We have used high resolution AFM based dynamic force spectroscopy to investigate peptide-lipid membrane interactions by measuring the detachment (last-rupture) force distribution, $P(F)$, and the corresponding force dependent rupture rate, $k(F)$, for two different peptides and lipid bilayers. The measured quantities, which differed considerably for different peptides, lipid-membranes, AFM tips (prepared under identical conditions), and retraction speeds of the AFM cantilever, could not be described in terms of the standard theory, according to which detachment occurs along a single pathway, corresponding to a diffusive escape process across a free energy barrier. In particular, the prominent retraction speed dependence of $k(F)$ was a clear indication that peptide-lipid membrane dissociation occurs stochastically along several detachment pathways. Thereby, we have formulated a general theoretical approach for describing $P(F)$ and $k(F)$, by assuming that peptide detachment from lipid membranes occurs, with certain probability, along a few dominant diffusive pathways. This new method was validated through a consistent interpretation of the experimental data. Furthermore, we have found that for moderate retraction speeds at intermediate force values, $k(F)$ exhibits catch-bond behavior (i.e. decreasing detachment rate with increasing force). According to the proposed model this behavior is due to the stochastic mixing of individual detachment pathways which do not convert or cross during rupture. To our knowledge, such catch-bond mechanism has not been proposed and demonstrated before for a peptide-lipid interaction.

Peptide-lipid interactions are essential for understanding numerous cellular processes and their mechanisms. Both experimental and theoretical study of these interactions is notoriously difficult due to the complexity of the system and the wide range of time and length scales involved. The magnitude of these interactions differs significantly with peptide and lipid species, as well as with solution conditions. A number of methods have been successfully applied to study peptide-lipid interactions¹. In particular, atomic force microscopy (AFM) based single-molecule force spectroscopy^{2–4} can be used to quantitatively probe the strength and range of peptide-lipid membrane interactions, by measuring the detachment (last rupture) force, F , through repeated AFM retraction experiments. The standard approach to interpret the measured histogram, $P(F)$, of the stochastic force, F , is to model the peptide-lipid membrane detachment as a diffusive escape process across a free energy barrier^{5–8}. This single detachment pathway model is characterized by (i) an energy parameter (barrier height ΔU_0), (ii) a geometric parameter (attraction range Δx_0), and (iii) a kinetic parameter (intrinsic escape rate k_0 , or escape time $\tau_0 = 1/k_0$). The values of the model parameters are determined by fitting the theoretical prediction to the experimental $P(F)$. While such an approach is applicable to other force-induced molecular transitions (e.g., unfolding of proteins^{9–14}, unzipping of nucleic acid hairpins^{15,16}, ligand-receptor dissociation^{17,18}, etc.), our experimental results indicate that the single detachment pathway model fails for peptide-lipid membrane systems, most likely due to their complexity. For such systems, $P(F)$ histograms show noticeable differences even for otherwise identically prepared samples, and depend strongly on other experimental factors, such as the retraction speed, v .

In general, whenever the single detachment pathway model is applicable, the force dependent detachment rate, $k(F)$, which can be obtained directly from the experimental histogram $P(F)$, is independent of v and increases

¹Department of Physics and Astronomy, University of Missouri, Columbia, MO, 65211, USA. ²Present address: Department of Anesthesiology, Weill Cornell Medicine, New York, NY, 10065, USA. ³Present address: Department of Physics and Astronomy, California State Polytechnic University, Pomona, CA, 91768, USA. ⁴Department of Biochemistry, University of Missouri, Columbia, MO, 65211, USA. Milica Utjesanovic and Tina R. Matin contributed equally. Correspondence and requests for materials should be addressed to G.M.K. (email: kinggm@missouri.edu) or I.K. (email: kosztini@missouri.edu)

monotonically with F ^{8,19}. Our experiments show that, for peptide-lipid membrane detachment, $k(F)$ depends strongly on the retraction speed and has non-monotonic behavior in F , thus implying that for such systems multiple detachment pathways are in play.

The purpose of this paper is to formulate and apply a general, multi-pathway model for describing the detachment force distribution, $P(F)$, and the corresponding $k(F)$, of forced detachment of peptides from lipid membranes. We demonstrate the viability of the proposed model by applying it to AFM retraction experiments, performed under different experimental conditions, that involve two different peptides (of different length) and two species of lipid bilayers. Our model assumes that the detachment process can proceed stochastically along a few, $N > 1$, dominant pathways, with probabilities w_n , $n = 1, \dots, N$, such that $\sum_{n=1}^N w_n = 1$. Similarly to the standard theory^{8,19}, each pathway is modeled as a diffusive escape process across a free energy barrier, characterized by the parameters ΔU_{0n} , Δx_{0n} and k_{0n} . We identify these pathways as final rupture events involving either one or two residues of the peptide. Indeed, due to its polymeric nature, the separation of the peptide from the membrane during retraction proceeds residue-by-residue. Right before detachment, the peptide-lipid membrane contact is restricted to a single residue, in general, located at the end of the peptide away from the AFM tip. Thus, depending on the time resolution of the AFM instrument, F extracted from the retraction force time series, corresponds to the dissociation of the last residue, or the dissociation in rapid succession of the last two (or more) residues still in contact with the membrane. Thus, approximate values of the peptide residue and lipid species specific energetic (ΔU_{0n}) and geometric (Δx_{0n}) parameters can be obtained from previous free energy profile studies of individual residue analogs interacting with model lipid membranes^{20,21}, leaving as effective fitting parameters only the intrinsic detachment rates k_{0n} and the pathway weight factors w_n . Furthermore, once the kinetic parameters (k_{0n}) have also been determined for a specific peptide and lipid-membrane system, by changing experimental conditions (e.g., modifying the retraction speed v , or exchanging - otherwise identically prepared - AFM tips) one only needs to tune the weights w_n in order to match the experimental $P(F)$ and $k(F)$ with the theoretical model. Indeed, in general, the probability that detachment follows a certain pathway should change by modifying the experimental conditions.

In spite of its formal simplicity, the proposed theoretical model is capable of describing, and interpreting in a consistent manner both $P(F)$ and $k(F)$ for all the different AFM retraction experiments reported here. In addition, we find that for intermediate retractions speeds and rupture forces, $k(F)$ exhibits “catch-bond” behavior^{22–24} when, counter intuitively, the detachment rate decreases with increasing F . We show that this behavior is due to properly weighted, force dependent contributions by different detachment pathways to $k(F)$. Another finding is that the intrinsic (detachment-) off-rate, $k_0 = k(0) = \sum_{n=1}^N w_n k_{0n}$, of the peptide from the membrane (within reasonable numerical errors) is independent of v , in spite of the fact that the forces w_n are v -dependent while k_{0n} are not.

It should be noted that, recently, others have also suggested that force-induced transitions in complex molecular systems should involve several reaction pathways, and presented detailed model calculations for different relevant scenarios²⁵. However, we are not aware of any study that uses a multiple detachment pathway approach to consistently describe and interpret single molecule dynamic force spectroscopy data, as reported here.

Theory

The forced detachment of a short peptide (biomolecule) from a lipid membrane (substrate), observed in AFM single-molecule dynamic force spectroscopy experiments (Fig. 1a), is a stochastic process that customarily is modeled as a diffusive escape event across a free energy barrier^{5–8}. The reaction coordinate, x , is defined as the separation between peptide and membrane, along the normal direction to the latter. In the absence of a pulling force, F , the intrinsic free energy profile (potential of mean force or PMF), $U_0(x)$, is characterized by the separation $\Delta x_0 = x_{\uparrow} - x_{\downarrow}$ between the positions of the equilibrium bound state (x_{\downarrow}) and transition state (x_{\uparrow}), and the barrier height (activation energy), ΔU_0 , separating these two states (see Fig. 1b). Here we model the PMF by a widely used linear-cubic potential $U_0(x) = \Delta U_0[(3/2)(x/\Delta x_0) - 2(x/\Delta x_0)^3]$, which was shown to be suitable for studying forced detachment processes⁸. In addition, the dynamics of the detachment process also depends on an effective diffusion coefficient, D , or, equivalently, an intrinsic escape rate k_0 , or escape time $\tau_0 = 1/k_0$.

In a constant pulling speed (force-ramp) AFM experiment, the applied force, $F(t)$, modifies the PMF, i.e., $U(x|F) = U_0(x) - Fx$, thus facilitating the detachment (last rupture) process by reducing both the barrier height, $\Delta U(F) < \Delta U_0$, and separation, $\Delta x(F) < \Delta x_0$ (Fig. 1b). The stochastic process $x(t)$ starts at (or about) x_{\downarrow} and terminates with detachment, when it reaches the absorbing boundary at x_{\uparrow} . The corresponding detachment force is also a stochastic quantity whose distribution function, $P(F)$, can be constructed from repeated AFM retraction experiments. Our goal is to determine the model parameters ΔU_0 , Δx_0 and k_0 that reproduce $P(F)$ obtained from single-molecule AFM force spectroscopy experiments. The theoretical approach for determining $P(F)$ requires several approximations that are discussed below.

Detachment along a single pathway. The key quantity for modeling molecular detachment processes along a given pathway is the survival probability (i.e., the probability that bonding is still intact at time t) defined as $S(t|z) = \int_a^b p(x, t|z) dx$, where $p(x, t|z)$ is the (transition) probability that the stochastic process $x(t)$ has the value x (with $a \leq x \leq b$) at time t , assuming that at $t = 0$ it had the sharp value $z \equiv x(0)$. In our case $z = x_{\downarrow}$, and there is an absorbing boundary at $b = x_{\uparrow}$, and a reflective boundary at $a < x_{\downarrow}$. When $U(x)$ diverges rapidly for $x < x_{\downarrow}$, one can set $a = -\infty$.

Because the transition probability obeys the adjoint Smoluchowski equation²⁶, $\partial_t p(x, t|z) = \mathcal{L}_S^\dagger(z) p(x, t|z)$, with $\mathcal{L}_S^\dagger(z) = D \exp[\beta U(z)] \partial_z \exp[-\beta U(z)] \partial_z = D \partial_z^2 - \beta D U'(z) \partial_z$, the equation of motion for the survival probability reads $\dot{S}(t|z) \equiv \partial_t S(t|z) = \mathcal{L}_S^\dagger(z) S(t|z)$, subject to the initial condition $S(0|z) = 1$, and boundary condition $S(t|x_{\uparrow}) = 0$. In general, $S(t|z)$ can be calculated only numerically. However, a practical analytical approximation can

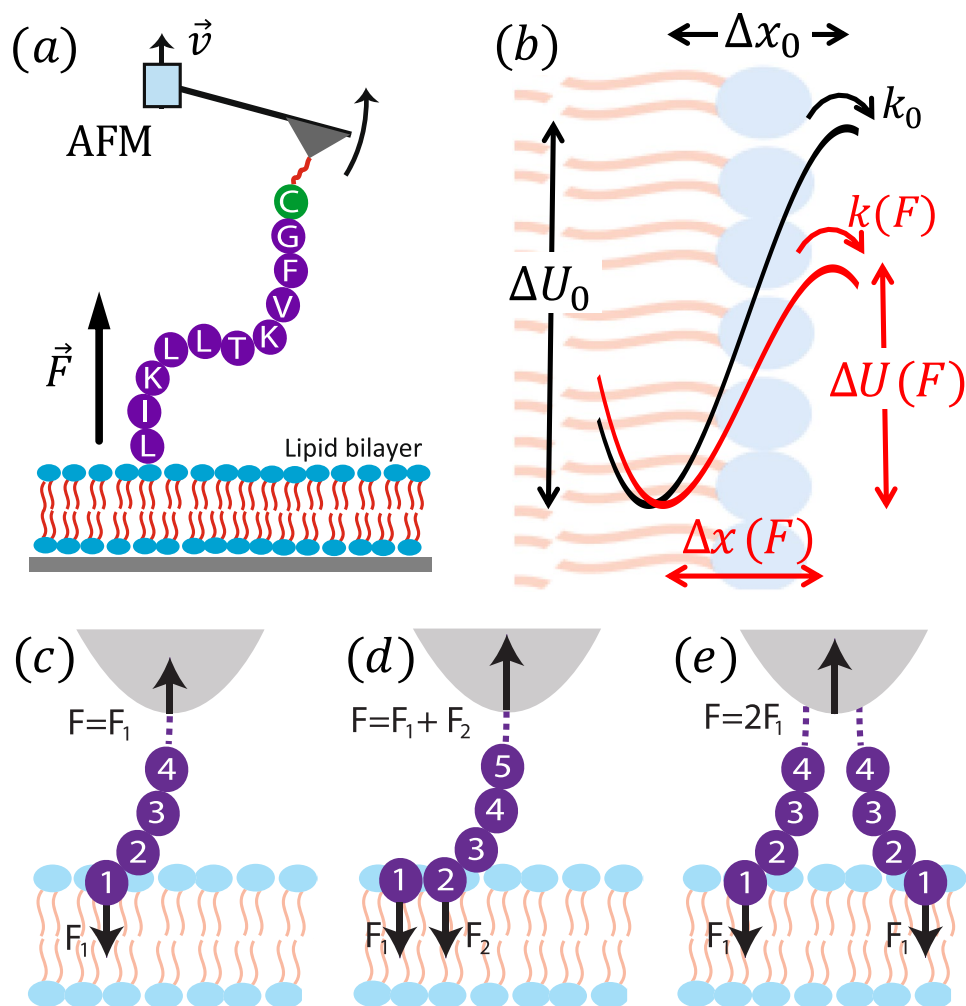


Figure 1. (a) Experimental setup showing SecA2-11 interacting with a supported lipid bilayer. (b) Physical model. Peptide detachment involves the (c) last amino acid (AA) or (d) last and next-to-last AA, or occasionally the (e) last two AA from neighboring peptide chains.

be obtained by employing the mean-detachment-time (MDT), or mean-first-passage-time (MFPT)²⁶ approximation. To this end, note that the distribution function of the detachment time is given by $\mathcal{P}(t) = -\dot{S}(t|z)$. Thus, the MDT, $\tau(z) = \int_0^\infty t \mathcal{P}(t) dt = \int_0^\infty S(t|z) dt$. Consequently, $\mathcal{L}_S^\dagger(z) \tau(z) = \int_0^\infty \mathcal{L}_S^\dagger(z) S(t|z) dt = \int_0^\infty \dot{S}(t|z) dt = -1$. This is the well-known MFPT equation, which can be integrated exactly with the result²⁶

$$\tau(z) = D^{-1} \int_z^{x_0} dx \exp[\beta U(x)] \int_a^x dy \exp[-\beta U(y)]. \quad (1)$$

Clearly, the (mean) detachment time $\tau = \tau(x_0)$. Note that in the large barrier limit, Eq. (1) turns into the widely used Kramers' formula for the escape time^{6,8,27,28}.

In general, the MDT (or quasi-adiabatic) approximation is applicable when τ is much larger than the characteristic relaxation time of the unruptured system. In single-molecule dynamic force AFM experiments, this approximation usually holds for sufficiently small force loading rates, $\dot{F} = dF/dt$. For simplicity, here we consider only constant loading rates, with $\dot{F} = k_s v$, where k_s is the stiffness of the AFM cantilever and v is the constant retraction speed. While the presence of the linker between the tip of the cantilever and biomolecule leads to a weak force dependence of \dot{F} , in many cases this dependence can be either neglected or accounted for through a mean spring constant $k_s^* \sim k_s$.

In the MDT approximation, the equation of motion for the survival probability is simplified, $\dot{S}(t) = \mathcal{L}_S^\dagger S(t) \approx -\tau^{-1} S(t) = -kS(t)$, and it can be integrated with the result $S(t) = \exp(-\int_0^t k dt')$. Finally, in terms of the survival probability, the rupture force distribution is $P(F) = -dS/dF = -\dot{S}/\dot{F}$, which in the MDT approximation becomes

$$P(F) = \frac{k(F)}{\dot{F}} S(F) = \frac{k(F)}{\dot{F}} \exp\left[-\int_0^F \frac{k(f)}{\dot{F}} df\right], \quad (2)$$

where the force dependent detachment rate $k(F) = 1/\tau(x_c)$, with the MDT given by Eq. (1). After little algebra, $k(F)$ can be expressed from Eq. (2) only in terms of the experimental histogram $P(F)$ and force loading rate, i.e.,

$$k(F) = \frac{\dot{F}P(F)}{1 - D(F)}, \quad D(F) = \int_0^F P(f)df. \quad (3)$$

Either of the last two equations can be used to determine the sought model parameters ΔU_0 , Δx_0 and k_0 , by fitting the theoretical prediction to the experimental data. However, Eq. (3) is crucial in determining whether the detachment process follows a single pathway or multiple pathways. Indeed, in the case of a single detachment pathway, $k(F)$ is independent of the retraction speed v . Thus, $k(F|v)$ obtained from AFM experiments using different retraction speeds must collapse to the same, monotonically increasing curve⁸. On the other hand, whenever $k(F|v)$ shows significant v dependence (and possibly non-monotonic behavior in F) it is a clear indication that the detachment process occurs stochastically along several different pathways.

Detachment along multiple pathways. It is natural to assume that the detachment of a peptide from a lipid membrane, due to the complex, stochastic nature of their interaction, may follow a number of different, independent pathways. In such case, the probability that detachment has not occurred yet at time t (survival probability) can be written as a weighted sum $S(t) = \sum_{n=1}^N w_n S_n(t)$, where w_n is the probability of detachment along the n -th pathway. Clearly, $\sum_{n=1}^N w_n = 1$. Each detachment pathway is characterized by the parameters ΔU_{0n} , Δx_{0n} and k_{0n} , $n = 1, \dots, N$. Using the MDT approximation described in the previous section, it is straightforward to show that, in the case of multiple pathways, the detachment force distribution can be written

$$P(F) = -\frac{dS}{dF} = \sum_{n=1}^N w_n P_n(F), \quad (4a)$$

where for the n -th pathway

$$P_n(F) = \frac{k_n(F)}{\dot{F}} S_n(F), \quad (4b)$$

with

$$S_n(F) = \exp\left[-\int_0^F \frac{k_n(f)}{\dot{F}} df\right]. \quad (4c)$$

Similarly to Eq. (1), the force dependent detachment rate for the n -th pathway

$$k_n(F) = D\left[\int_{x_{n\cup}}^{x_{n\cap}} dx \exp[\beta U_n(x)] \int_{-\infty}^x dy \exp[-\beta U_n(y)]\right]^{-1}, \quad (5)$$

and the corresponding intrinsic detachment rate $k_{0n} = k_n(0)$. Equations (4), together with Eq. (5), are the multiple pathways equivalent of Eq. (2), and can be used to determine the model parameters ΔU_{0n} , Δx_{0n} and k_{0n} , along with the weight factors w_n , by fitting the experimental data.

Finally, the mean, force dependent, detachment rate for multiple pathways is given formally by the same Eq. (3) as for a single detachment pathway, except that for $P(F)$ one needs to use Eq. (4). Thus

$$k(F) = \sum_{n=1}^N \alpha_n(F) k_n(F), \quad \alpha_n(F) = \frac{w_n S_n(F)}{\sum_{n=1}^N w_n S_n(F)}. \quad (6)$$

Depending on the pathways involved, due to the force dependence of the $\alpha_n(F)$ coefficients, $k(F)$ may depend strongly on the retraction speed, v , and may also exhibit non-monotonic dependence (i.e., *catch-bond* behavior²²) on the detachment force, F .

Double and multiple detachment events. In many cases, right before detachment, the contact between a peptide and lipid membrane is confined to a single amino acid (Fig. 1c), and the experimentally recorded detachment (last rupture) force corresponds to such situation. However, due to the limited time resolution of the AFM or other experimental complications, occasionally the recorded detachment force corresponds to a double rupture event, e.g., when either the last two amino acids of a single peptide (Fig. 1d), or the last amino acids of two copies of the peptide (attached to the tip of the AFM cantilever; Fig. 1e), in contact with the membrane, rupture in rapid succession. In double rupture cases, the measured detachment force is roughly twice as big as for the corresponding single detachment event. Thus, double rupture events can be regarded as independent detachment pathways with a weight factor $w_m^{(2)}$ and a rupture force distribution $P_m^{(2)}(F) = (1/2)P_m(F/2)$, where $P_m(F) \equiv P_m^{(1)}(F)$ corresponds to single residue detachment. In principle, one may consider multiple detachment events that involve the rupture in rapid succession (that cannot be time-resolved experimentally) of $p > 2$ amino acids, which can be modeled as pathways with $w_n^{(p)}$ and $P_m^{(p)}(F) = (1/p)P_m(F/p)$. However, the occurrence of multiple detachment events with $p > 2$ is much smaller than those involving single and double ruptures, and usually can be neglected.

Residue	$\Delta U_0 [k_B T]$	Δx_0 [nm]
L	8.0	1.0
I	10.0	1.3
S	2.0	0.7
R	8.2	1.3

Table 1. PMF model parameters describing the interaction of selected residues with POPC lipid bilayer^{20,21}.

AFM Experiments

Following our group's recent work, high precision AFM-based single molecule force spectroscopy experiments were performed to measure the detachment (last rupture) force between two different peptides and two lipid bilayer species². Peptides were derived from SecA, which is a large (901 amino acid) peripheral membrane protein central to the general Sec system. We focused on two distinct segments of SecA: the extreme N-terminal 10 amino acids (SecA2-11) as well as a 20 amino acid segment in the middle of the protein (SecA600-619). The membrane bilayer was varied between 1-palmitoyl-2-oleoyl-sn-glycero-3-phosphocholine (POPC) which is a model zwitterionic lipid and *E. coli* polar lipid which is a mixture of zwitterionic (phosphatidylethanolamine) and charged (phosphatidylglycerol and cardiolipin) lipids (all lipids were purchased from Avanti).

Peptides were synthesized in house using solid-phase synthesis on Sieber amide resin and standard Fmoc/tBu chemistry for linear elongation resulting in purities $\geq 95\%$ with the follow sequences: SecA600-619: SDRVSGMMRKLGMKPGEAIE-C and SecA2-11: LIKLLTKVFG-C. The cysteine residue at the C-terminus of both peptides allowed site-specific, covalent functionalization onto AFM tips via a 9.5 nm long PEG linker. Incubation conditions were optimized to yield ~ 1 peptide tethered at the tip apex, as described previously^{2,29}. To allow pN level precision, we utilized bioleover long cantilevers (Olympus) without metallic coatings³⁰. Cantilever spring constants (k_s) were in the range of 3–8 pN/nm, determined via the thermal calibration. Supported bilayers were formed by vesicle fusion to clean glass surfaces³¹ which were rinsed (0.1 mL buffer solution, 3x) prior to force spectroscopy experiments. Such conditions result in uniform bilayer coverage over large areas^{2,31}.

Force spectroscopy experiments were carried out in aqueous buffer solution (10 mM Hepes pH 7.6, 300 mM KAc, 5 mM Mg(Ac)₂) at $\sim 30^\circ$ using a commercial AFM (Cypher, Asylum Research). The speed, v , was controlled by the piezoelectric stage affixed to the base of the cantilever. Rupture forces > 60 pN were rare and excluded from analysis. Additionally, rupture events occurring < 3 nm above the lipid surface were excluded (to minimize non-specific interactions). Unless otherwise specified, for each experimental condition, data from ≥ 5 distinct tips were aggregated, yielding between 275–529 distinct rupture events per condition.

Results and Discussion

In a series of high precision AFM-based single molecule force spectroscopy experiments we have measured repeatedly, under different experimental conditions, the (stochastic) peptide-lipid membrane detachment force, F , using two different peptides (SecA2-11 and SecA600-619) and two lipid (zwitterionic POPC and charged *E. coli* polar) membranes. The constructed $P(F)$ histograms showed significant variation from experiment to experiment, even for the same peptide-lipid membrane system. Attempts to model $P(F)$ by using the theory for a single detachment pathway failed. We attribute this failure to the complexity of the peptide-lipid membrane interactions. Here we show that in fact $P(F)$ can be modeled in a consistent way by assuming that peptide-lipid membrane detachment involves a small number (usually $N = 3$ or 4) of dominant pathways of single and double rupture events. The modeling strategy is as follows. First, one identifies the residues at the end of the peptide that are most likely to rupture last. For SecA2-11 (SecA600-619) these residues are L and I (S, D, and R). Next, the corresponding values of the PMF parameters, ΔU_{0n} and Δx_{0n} , are identified from previous MD simulation studies^{20,21}, which reconstructed the PMF of various residues interacting with POPC bilayers. These values are listed in Table 1. Finally, the intrinsic detachment rates k_{0n} (kinetic parameters) and occurrence probabilities w_n (weight coefficients) for each participating detachment pathway ($n = 1, \dots, N$) are determined by fitting the experimental $P(F)$ histograms using Eqs (4) and (5). It should be emphasized that the PMF parameters (ΔU_{0n} and Δx_{0n}) are determined by the nature of the peptide and lipid membrane and, thus, their values should not be changed during the fitting process. Also, one expects that the rates k_{0n} may depend slightly on the experimental conditions (e.g., retraction speed v , AFM cantilever tip), but not as much as the weight factors w_n , which may change considerably from experiment to experiment. While the convergence of w_n to a peptide-lipid membrane specific value may require a very large number of measurements, the parameters identifying the individual pathways (i.e., ΔU_{0n} , Δx_{0n} , and k_{0n}) should be obtainable from a relatively small number of single molecule experiments.

Next, we consider three exemplary cases to demonstrate the viability of the method described above for interpreting detachment force histograms for peptide-lipid membrane systems.

$P(F)$: AFM-tip dependence. The experimental $P(F)$ histogram of SecA2-11 interacting with POPC lipid bilayer (for $v = 100$ nm/s) shown in Fig. 2a can be fitted well by assuming $N = 4$ detachment pathways. The quality of this fit, as well as the other $P(F)$ fits reported in this paper, is rather good, characterized by a coefficient of determination $R^2 > 0.9$. Two of these ($n = 1, 2$) are identified as single ruptures involving the last two residues, L and I, of the peptide. The other two pathways ($n = 3, 4$) correspond to double rupture processes involving the same residues. The corresponding PMF parameters are listed in Table 1, while the fitting parameters, k_{0n} and w_n , are listed in Fig. 2a. Note that, in this case, the single rupture events (65%) are more prevalent than double ruptures (33%).

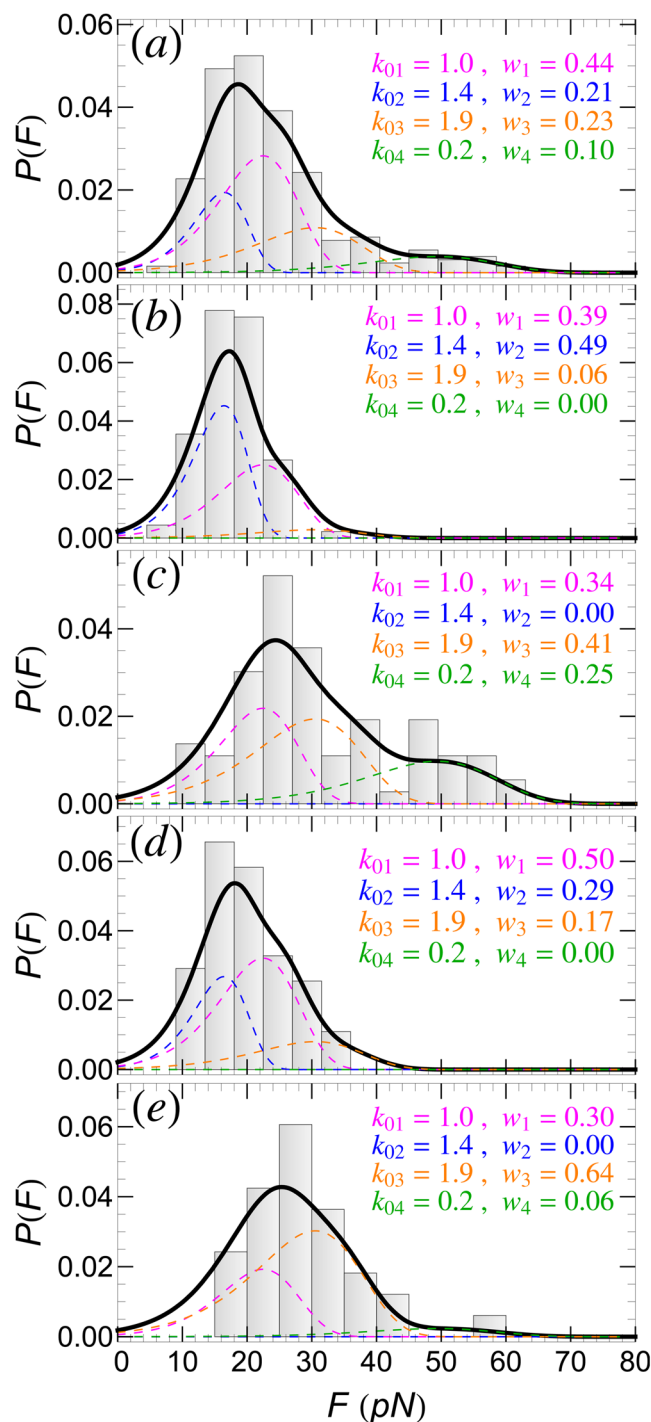


Figure 2. Detachment force histogram, $P(F)$, of SecA2-11 interacting with POPC bilayer using data from (a) all AFM tips, and (b–e) four individual AFM tips. In each case, $P(F)$ can be fitted well by using four detachment pathways. Contributions to $P(F)$ from the n -th ($n = 1, \dots, 4$) detachment pathways are shown as colored dashed curves; the corresponding intrinsic rupture rates, k_{0n} , and weights, w_n , are also listed.

Also, the predominant four pathways account for 98% of $P(F)$; the remaining 2% correspond to other pathways that occur only seldom and, thus, can be neglected.

The $P(F)$ histogram in Fig. 2a contains data from several AFM retraction experiments, performed with different, but otherwise identically prepared, AFM tips. Reflecting the stochastic nature of single molecule experiments, the $P(F)$ histograms for individual tips, shown in Fig. 2b–e, have completely different shapes. However, all these different histograms can be well fitted assuming the same $N = 4$ detachment pathways identified above, but with different weight factors w_n . This means that, in otherwise identically prepared samples, certain detachment pathways may be favored against others. While, in general, one cannot predict the prevalence of a particular

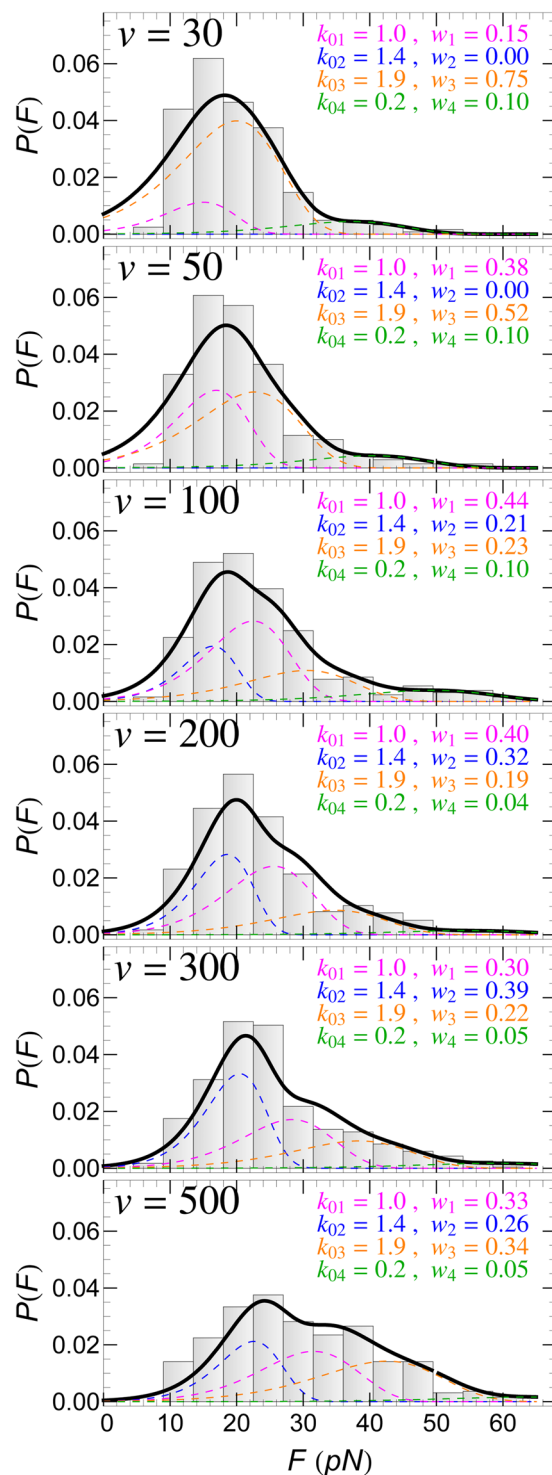


Figure 3. Detachment force histogram, $P(F)$, of SecA2-11 interacting with POPC bilayer for different retraction speeds (in nm/s) of the AFM tip. In each case, $P(F)$ can be fitted well by using four detachment pathways (solid-thick curves). Contributions to $P(F)$ from the n -th ($n = 1, \dots, 4$) detachment pathways are shown as colored dashed curves; the corresponding intrinsic rupture rates, k_{0n} , and weights, w_n , are also listed.

pathway in individual experiments, it is still remarkable that $P(F)$ can be reproduced by only using w_n 's as actual fitting parameters. Thus, the detachment pathways, identified through three parameters (i.e., ΔU_{0n} , Δx_{0n} , and k_{0n}), can be regarded as fingerprints of a specific peptide-lipid membrane system.

$P(F)$: retraction speed, v , dependence. The experimental $P(F)$ histogram of SecA2-11 interacting with POPC lipid bilayer for six different retractions speeds are shown in Fig. 3. In all these cases too, $P(F)$ can be fitted

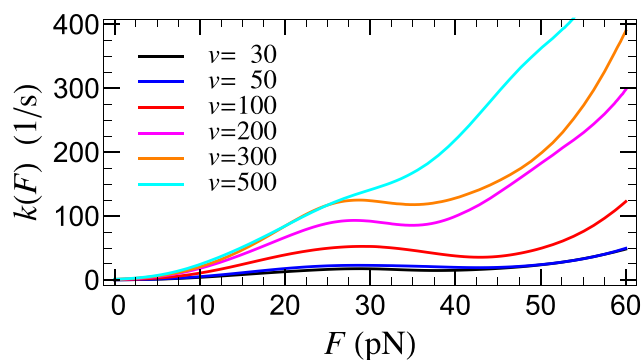


Figure 4. Force dependent detachment rate, $k(F)$, determined from Eq. (3), for SecA2-11 interacting with POPC bilayer, for the listed retraction speeds (in nm/s) of the AFM tip.

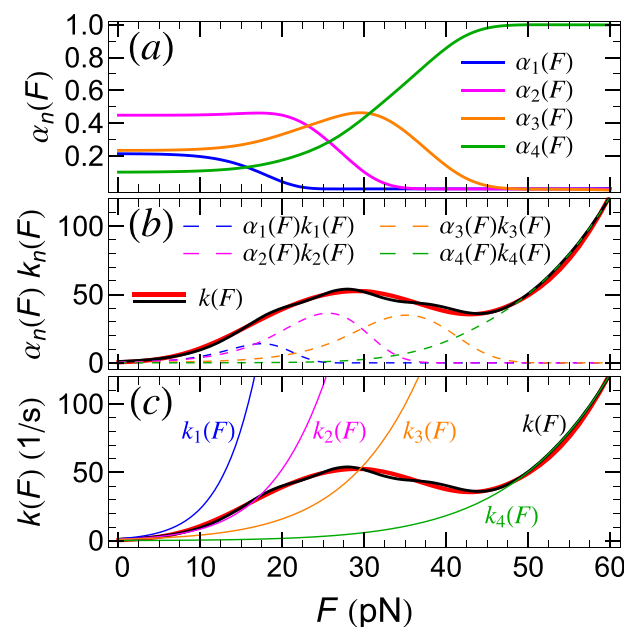


Figure 5. Force dependent detachment rate, $k(F)$, of SecA2-11 from POPC lipid bilayer obtained from AFM retraction experiments with $v = 100$ nm/s retraction speed. (a) Force dependent weight factors for each detachment pathway. (b) $k(F)$ derived using $P(F)$ from experiment (thick, solid red curve) and our theoretical modeling (solid black curve). The weighted contributions of individual pathways to $k(F)$, i.e., $\alpha_n(F)k_n(F)$, $n = 1, \dots, 4$, are also shown (dashed curves). (c) Pathway specific, force dependent rupture rates, $k_n(F)$. For reference, the experimental and theoretical $k(F)$ are also shown as in (b).

well by assuming the same four detachment pathways identified in the previous section, and by simply adjusting the corresponding weight factors w_n . It appears that for the lowest retraction speeds, $v = 30$ and 50 nm/s, the double rupture pathways are the dominant ones, accounting respectively for 85% and 62% of $P(F)$. For higher speeds, the situation is reversed, in favor of the single rupture pathways.

As already mentioned, the strong v dependence of $k(F)$, determined from the experimental $P(F)$ by means of Eq. (3), and shown in Fig. 4, clearly demonstrates that peptide-lipid bilayer detachment cannot be described by a single detachment pathway, thus lending support to our multiple pathways method. While the individual rates, $k_n(F)$, for each detachment pathway are monotonically increasing with F , the non-monotonic behavior of $k(F)$, given by Eq. (6), is due to the F -dependent contributions [through the coefficients $\alpha_n(F)$] of the individual pathways. The situation is illustrated, for $v = 100$ nm/s, in Fig. 5.

It is remarkable that, for intermediate forces, the stochastic mixing between the different pathways may lead to “catch-bond” behavior^{22–24}, where counter-intuitively the detachment rate decreases with the increase of the applied force (Fig. 5b). To the best of our knowledge, this is the first time when a catch-bond mechanism based on detachment pathway mixing has been proposed and demonstrated for a peptide-lipid membrane interaction. It should be emphasized that the origin of the catch-bond in this case is quite different from the so-called (phenomenological) “two-pathway” model, according to which catch-bond behavior in ligand-receptor systems comes about through pathway switching (inner conversion)²⁴. Here, individual peptide-lipid detachment events occur,

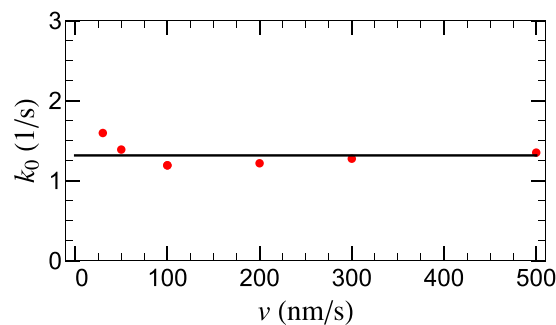


Figure 6. AFM retraction speed, v , dependence of the intrinsic detachment rate, $k_0 = k(F=0)$, (red filled-circles) of SecA2-11 interacting with POPC bilayer. Horizontal black line represents the mean value (k_0).

with a given probability, along well defined pathways, which do not cross or convert during rupture. Thus, the origin of the catch-bond behavior in peptide-lipid membrane interaction is due to the experimental inseparability of the multiple pathways along which detachment may occur. While the contribution of individual pathways to $P(F)$ are force independent (w_n), the weight of the same contribution (α_n) to the effective detachment rate $k(F)$ decreases with force because fewer attachments are still intact (see also Fig. 5a and Eq. (6)). For sufficiently large forces, when only two pathways contribute to $k(F)$, the latter should exhibit, in a narrow force range, catch-bond behavior with $dk/dF < 0$ (see Fig. 5).

Furthermore, it is also remarkable that, in spite of the significant v -dependence of $P(F)$ and $k(F)$, the intrinsic (detachment) off-rate, $k_0 = k(0) = \sum_{n=1}^4 w_n k_{0n} \approx 1.2 \text{ s}^{-1}$, obtained from Eq. (6) for $F=0$, appears to be independent of v , as shown in Fig. 6. This, normally expected but non-trivial result, lends further support to our theoretical model.

$P(F)$: peptide and membrane dependence. Finally, we demonstrate that the proposed multiple detachment pathways method works equally well for other peptides and types of lipid bilayers.

First, consider the detachment of SecA600-619 interacting with POPC (for the same $v=100 \text{ nm/s}$ as for SecA2-11). The last three residues of this peptide are S, D and R. Previous MD simulation studies^{20,21} have shown that there is essentially no escape barrier for D interacting with POPC, and the one for S is negligibly small (see Table 1). Therefore, in order to fit the experimental $P(F)$ histogram, one needs to consider two single rupture pathways, associated with residue R (with two different intrinsic rates, k_{01} and k_{02}), along with a third, double rupture pathway that involves two R residues. Similarly to SecA2-11, as shown in Fig. 7a, the experimental $P(F)$ for SecA600-619 can be fitted well with the theoretical model involving the above three pathways. The values of the fitting parameters, k_{0n} and w_n , are listed in the same figure.

As shown in Fig. 7b, the experimental $P(F)$ for SecA600-619 interacting with an *E. coli* membrane deviates significantly from the one with POPC bilayer (Fig. 7a). However, in this case too, the same three detachment pathways as for POPC can be used to fit $P(F)$, by keeping the same (residue specific) PMF parameters but, re-evaluating (as fitting parameters) both the intrinsic kinetic rates k_{0n} and the weight factors w_n . These new values are listed in Fig. 7b. The justification for keeping the same ΔU_{0n} and Δx_{0n} for *E. coli* as for POPC is twofold: (i) the lack of PMF data for peptide residues in *E. coli* membrane, and (ii) the fact that in *E. coli* membrane the zwitterionic lipids are more abundant (~70%) than the anionic ones (~30%). It appears, however, that the presence of charged lipids in the *E. coli* membrane leads to a considerable increase of both the rates k_{0n} , and the frequency of double rupture detachment events at the expense of single ruptures.

Conclusions

We have used high resolution AFM-based dynamic force spectroscopy to investigate quantitatively peptide-lipid membrane interactions by measuring the detachment (last-rupture) force distribution, $P(F)$, and the corresponding force dependent rupture rate, $k(F)$, for two different peptides (SecA2-11 and SecA600-619) and lipid bilayers (zwitterionic POPC and charged *E. coli* polar membrane). The measured quantities, which differed considerably for different peptides, lipid-membranes, AFM tips (prepared under identical conditions), and retraction speeds of the AFM cantilever, could not be described in terms of the standard theory that assumes that detachment occurs along a single pathway. In particular, the prominent v -dependence of $k(F)$ was a clear indication that peptide-lipid membrane detachment occurs stochastically along several detachment pathways.

A main result of this work is the formulation and validation of a general theoretical approach that provides a quantitative description of the detachment force distribution of a peptide from a lipid membrane. The proposed model assumes that detachment occurs, with certain probability (w_n), along a few dominant diffusive pathways, characterized by three parameters (ΔU_{0n} , Δx_{0n} , and k_{0n}). We have identified these pathways with last-rupture events involving one or two residues, in general, located at the end of the peptide. The values of the energetic (ΔU_{0n}) and geometric (Δx_{0n}) parameters, which are residue and lipid species specific, were derived from existing free energy profile studies, while the kinetic parameters (k_{0n}) and pathway weights (w_n) were used as fitting parameters. This new theoretical approach allowed for a consistent interpretation of all our experimental data. Interestingly, even for the same peptide-lipid membrane system, the occurrence frequency of different dominant detachment pathways (measured through w_n) showed significant AFM tip dependence, although these tips were

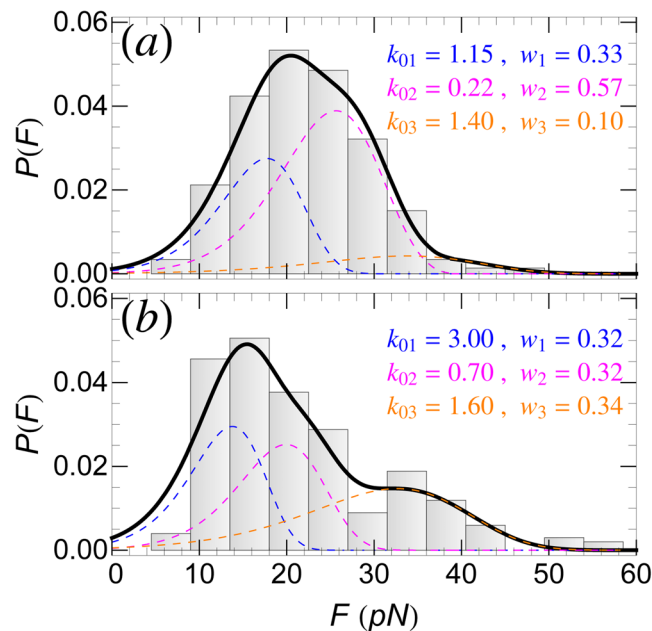


Figure 7. Detachment force histogram, $P(F)$, of SecA600-619 peptide interacting with (a) POPC bilayer, and (b) *E. coli* membrane. $P(F)$ can be fitted well by using three detachment pathways (solid-thick curves). Contributions to $P(F)$ from the n -th ($n = 1, \dots, 3$) detachment pathways are shown as colored dashed curves; the corresponding intrinsic rupture rates, k_{0n} , and weights, w_n , are also listed.

prepared identically. However, even if one cannot predict the occurrence probability of a particular pathway in individual experiments, it is quite remarkable that, once the pathways have been identified and characterized, the rupture force histogram $P(F)$ can be matched by only using w_n 's as fitting parameters.

Our theoretical model also reproduced accurately both retraction speed and non-monotonic force dependence of the rupture rate $k(F)$. For moderate v and intermediate F values, $k(F)$ exhibited *catch-bond* behavior, namely a decrease with increasing F , before continuing to increase again, as normally expected. According to our model, the origin of the catch-bond mechanism in peptide-lipid membrane interactions is the stochastic mixing of individual detachment pathways, which do not convert or cross during rupture. This catch-bond mechanism is manifestly different from the commonly used “two-pathway” model²⁴ for ligand-receptor systems.

Using our theoretical model, we also calculated the intrinsic detachment (or off) rate, $k(0) = \sum_{n=1}^N w_n k_{0n}$, of the peptide SecA2-11 from the lipid bilayer POPC. As expected, the result was independent (within margin of errors) of the retraction speed, which is quite remarkable if we take into account that the pathway weights w_n are v -dependent while the individual rates k_{0n} are not.

To conclude, we notice that, beside the detachment (last rupture) forces, the retraction force time series, $F(t)$, contains detailed information about the entire peptide-lipid membrane interaction process, including intermediate rupture events. In the framework of our theoretical approach, the latter may be regarded as detachment events of intermediate residues. However, further work is needed to apply and test our theory for such intermediate rupture events.

References

- Simon, S. & McIntosh, T. *Peptide-Lipid Interactions*, vol. 52 of *Current Topics in Membranes* (Academic Press, 2002).
- Matin, T. *et al.* Single-molecule peptide-lipid affinity assay reveals interplay between solution structure and partitioning. *Langmuir* **33**, 4057–4065, <https://doi.org/10.1021/acs.langmuir.7b00100> (2017).
- Schwierz, N., Krysiak, S., Hugel, T. & Zacharias, M. Mechanism of reversible peptide-bilayer attachment: Combined simulation and experimental single-molecule study. *Langmuir* **32**, 810–821, <https://doi.org/10.1021/acs.langmuir.5b03435> (2016).
- Andre, G., Brasseur, R. & Dufrene, Y. F. Probing the interaction forces between hydrophobic peptides and supported lipid bilayers using afm. *J Mol Recognit* **20**, 538–45, <https://doi.org/10.1002/jmr.837> (2007).
- Bell, G. I. Models for the specific adhesion of cells to cells. *Science* **200**, 618–627, <https://doi.org/10.1126/science.347575> (1978).
- Evans, E. & Ritchie, K. Dynamic strength of molecular adhesion bonds. *Biophysical Journal* **72**, 1541–1555, [https://doi.org/10.1016/S0006-3495\(97\)78802-7](https://doi.org/10.1016/S0006-3495(97)78802-7) (1997).
- Hummer, G. & Szabo, A. Kinetics from Nonequilibrium Single-Molecule Pulling Experiments. *Biophysical Journal* **85**, 5–15, [https://doi.org/10.1016/S0006-3495\(03\)74449-X](https://doi.org/10.1016/S0006-3495(03)74449-X) (2003).
- Dudko, O. K., Hummer, G. & Szabo, A. Intrinsic Rates and Activation Free Energies from Single-Molecule Pulling Experiments. *Phys. Rev. Lett.* **96**, 108101–4, <https://doi.org/10.1103/PhysRevLett.96.108101> (2006).
- Cecconi, C., Shank, E. A., Bustamante, C. & Marqusee, S. Direct Observation of the Three-State Folding of a Single Protein Molecule. *Science* **309**, 2057–2060, <https://doi.org/10.1126/science.1116702> (2005).
- Kellermayer, M. S. Z., Smith, S. B., Granzier, H. L. & Bustamante, C. Folding-Unfolding Transitions in Single Titin Molecules Characterized with Laser Tweezers. *Science* **276**, 1112–1116, <https://doi.org/10.1126/science.276.5315.1112> (1997).
- Marszalek, P. E. *et al.* Mechanical unfolding intermediates in titin modules. *Nature* **402**, 100–103, <https://doi.org/10.1038/47083> (1999).

12. Rief, M., Gautel, M., Oesterhelt, F., Fernandez, J. M. & Gaub, H. E. Reversible Unfolding of Individual Titin Immunoglobulin Domains by AFM. *Science* **276**, 1109–1112, <https://doi.org/10.1126/science.276.5315.1109> (1997).
13. Schlierf, M., Li, H. & Fernandez, J. M. The unfolding kinetics of ubiquitin captured with single-molecule force-clamp techniques. *PNAS* **101**, 7299–7304, <https://doi.org/10.1073/pnas.0400033101> (2004).
14. Schlierf, M. & Rief, M. Single-Molecule Unfolding Force Distributions Reveal a Funnel-Shaped Energy Landscape. *Biophys J* **90**, L33–L35, <https://doi.org/10.1529/biophysj.105.077982> (2006).
15. Greenleaf, W. J., Frieda, K. L., Foster, D. A. N., Woodside, M. T. & Block, S. M. Direct Observation of Hierarchical Folding in Single Riboswitch Aptamers. *Science* **319**, 630–633, <https://doi.org/10.1126/science.1151298> (2008).
16. Liphardt, J., Onoa, B., Smith, S. B., Tinoco, I. & Bustamante, C. Reversible Unfolding of Single RNA Molecules by Mechanical Force. *Science* **292**, 733–737, <https://doi.org/10.1126/science.1058498> (2001).
17. Florin, E. L., Moy, V. T. & Gaub, H. E. Adhesion forces between individual ligand-receptor pairs. *Science* **264**, 415–417, <https://doi.org/10.1126/science.8153628> (1994).
18. Merkel, R., Nassoy, P., Leung, A., Ritchie, K. & Evans, E. Energy landscapes of receptor–ligand bonds explored with dynamic force spectroscopy. *Nature* **397**, 50–53, <https://doi.org/10.1038/16219> (1999).
19. Dudko, O. K., Hummer, G. & Szabo, A. Theory, analysis, and interpretation of single-molecule force spectroscopy experiments. *PNAS* **105**, 15755–15760, <https://doi.org/10.1073/pnas.0806085105> (2008).
20. MacCallum, J. L., Bennett, W. F. D. & Tieleman, D. P. Distribution of Amino Acids in a Lipid Bilayer from Computer Simulations. *Biophys J* **94**, 3393–3404, <https://doi.org/10.1529/biophysj.107.112805> (2008).
21. Pogorelov, T. V., Vermaas, J. V., Arcario, M. J. & Tajkhorshid, E. Partitioning of Amino Acids into a Model Membrane: Capturing the Interface. *The Journal of Physical Chemistry B* **118**, 1481–1492, <https://doi.org/10.1021/jp4089113> (2014).
22. Marshall, B. T. *et al.* Direct observation of catch bonds involving cell-adhesion molecules. *Nature* **423**, 190–193, <https://doi.org/10.1038/nature01605> (2003).
23. Evans, E., Leung, A., Heinrich, V. & Zhu, C. Mechanical switching and coupling between two dissociation pathways in a P-selectin adhesion bond. *PNAS* **101**, 11281–11286, <https://doi.org/10.1073/pnas.0401870101> (2004).
24. Pereverzev, Y. V., Prezhdo, O. V., Forero, M., Sokurenko, E. V. & Thomas, W. E. The Two-Pathway Model for the Catch-Slip Transition in Biological Adhesion. *Biophysical Journal* **89**, 1446–1454, <https://doi.org/10.1529/biophysj.105.062158> (2005).
25. Pierce, C. A. & Dudko, O. K. Distinguishing Signatures of Multipathway Conformational Transitions. *Physical Review Letters* **118**, <https://doi.org/10.1103/PhysRevLett.118.088101> (2017).
26. Risken, H. *The Fokker-Planck Equation: Methods of Solution and Applications*, 3rd edn (Springer-Verlag Telos, 1996).
27. Kramers, H. A. Brownian motion in a field of force and the diffusion model of chemical reactions. *Physica* **7**, 284–304, [https://doi.org/10.1016/S0031-8914\(40\)90098-2](https://doi.org/10.1016/S0031-8914(40)90098-2) (1940).
28. Hänggi, P., Talkner, P. & Borkovec, M. Reaction-rate theory: Fifty years after Kramers. *Rev. Mod. Phys.* **62**, 251, <https://doi.org/10.1103/RevModPhys.62.251> (1990).
29. Zimmermann, J. L., Nicolaus, T., Neuert, G. & Blank, K. Thiol-based, site-specific and covalent immobilization of biomolecules for single-molecule experiments. *Nat Protoc* **5**, 975–85 (2010).
30. Churnside, A. B. *et al.* Routine and timely sub-piconewton force stability and precision for biological applications of atomic force microscopy. *Nano Lett* **12**, 3557–61, <https://doi.org/10.1021/nl301166w> (2012).
31. Chada, N. *et al.* Glass is a viable substrate for precision force microscopy of membrane proteins. *Scientific Reports* **5**, 12550, <https://doi.org/10.1038/srep12550> (2015).

Acknowledgements

Work supported by the Burroughs Wellcome Fund (Career Award at the Scientific Interface), the NSF (CAREER Award #: 1054832), and the MU Research Board. The computation for this work was performed on the high HPC infrastructure provided by RCSS and in part by the NSF under grant number CNS-1429294 at the University of Missouri, Columbia MO.

Author Contributions

T.R.M. performed the experiments and analyzed the experimental data. K.P.S. performed experiments. T.R.M., K.P.S., and G.M.K. conceived the experiments. I.K. developed the theoretical model. M.U. and I.K. performed the theoretical analysis of the data. I.K. and G.M.K. wrote the manuscript. All authors reviewed the manuscript.

Additional Information

Competing Interests: The authors declare no competing interests.

Publisher's note: Springer Nature remains neutral with regard to jurisdictional claims in published maps and institutional affiliations.



Open Access This article is licensed under a Creative Commons Attribution 4.0 International License, which permits use, sharing, adaptation, distribution and reproduction in any medium or format, as long as you give appropriate credit to the original author(s) and the source, provide a link to the Creative Commons license, and indicate if changes were made. The images or other third party material in this article are included in the article's Creative Commons license, unless indicated otherwise in a credit line to the material. If material is not included in the article's Creative Commons license and your intended use is not permitted by statutory regulation or exceeds the permitted use, you will need to obtain permission directly from the copyright holder. To view a copy of this license, visit <http://creativecommons.org/licenses/by/4.0/>.

© The Author(s) 2019